

## Observations of Interplanetary Scintillations at 327 MHz

*A. Pramesh Rao*,<sup>A</sup> *S. M. Bhandari*<sup>B</sup> and *S. Ananthkrishnan*<sup>A</sup>

<sup>A</sup> Radio Astronomy Centre, Tata Institute of Fundamental Research,  
P. Box 8, Ootacamund 643001, India.

<sup>B</sup> Physical Research Laboratory, Ahmedabad 380009, India.

### *Abstract*

The properties of the interplanetary medium and the structures of 9 compact radio sources have been derived from the observed interplanetary scintillations at 327 MHz using the Ooty radio telescope. The observed scale size of the electron density irregularities has a value of 100 km in the elongation range 0.3-0.7 A.U. and shows no indication of increasing with elongation, as has been suggested by Hewish and Symonds (1969). The Bessel transforms of intensity fluctuations could seldom be used for estimating the solar wind velocity since the minima corresponding to the Fresnel filtering effect were rarely seen. The study of the skewness parameter of the probability distribution of intensity fluctuations at 327 MHz indicates that for elongations between 0.2 and 0.35 A.U. the thin screen model is satisfactory, but for larger elongations no clear conclusion can be drawn.

### 1. Introduction

The study of interplanetary scintillations (IPS) has yielded information on the properties of the interplanetary medium and also on the structures of radio sources with angular diameters between  $0''\cdot01$  and  $0''\cdot5$ . In this paper we report a systematic series of IPS observations of nine compact sources at 327 MHz using the Ooty radio telescope (Swarup *et al.* 1971). The observations were made mainly to study the properties of the interplanetary medium at 327 MHz. The results have been used to derive the structures of 194 radio sources in the southern sky from a further IPS survey (Bhandari *et al.* 1974, present issue pp. 121-8). The nine sources studied here are 3C2, PKS0115-01, PKS0116+08, 3C49, NRAO91, CTA21, 3C138, PKS2203-18 and 3C446.

Observations were carried out for  $p$ , the distance of closest approach of the line of sight to the source from the Sun, in the range 0.1-1.0 A.U. At 327 MHz the observations for  $p > 0.25$  A.U. lie in the weak scattering regime. In this regime we have derived the r.m.s. phase fluctuations produced by the interplanetary medium along the line of sight and the scale sizes of the irregularities, and the results, along with their variation with distance from the Sun, are presented in Section 3. In Section 4 we estimate the Bessel transforms of the intensity fluctuations and discuss the possible reasons for the rare occurrence of deep minima corresponding to the Fresnel filtering effect. A study of the skewness of the probability distribution of the intensity fluctuations is presented in Section 5. The structure of the nine observed sources is given in the last section.

### 2. Observation and Analysis

The observations were made during February to July 1971 using the Ooty radio telescope, which operates at 326.5 MHz and has a collecting area of 8700 m<sup>2</sup>. The

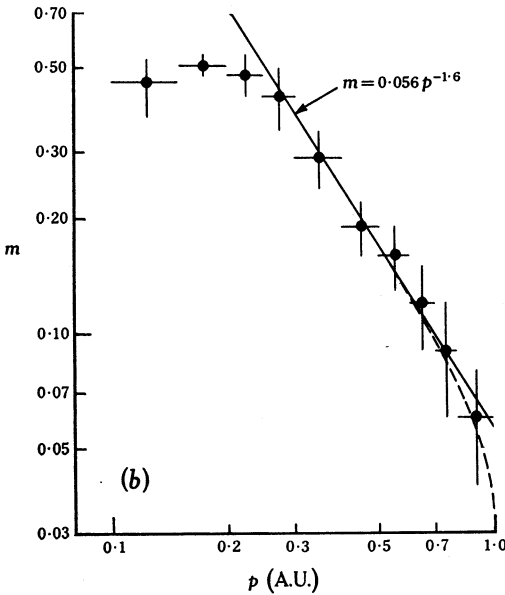
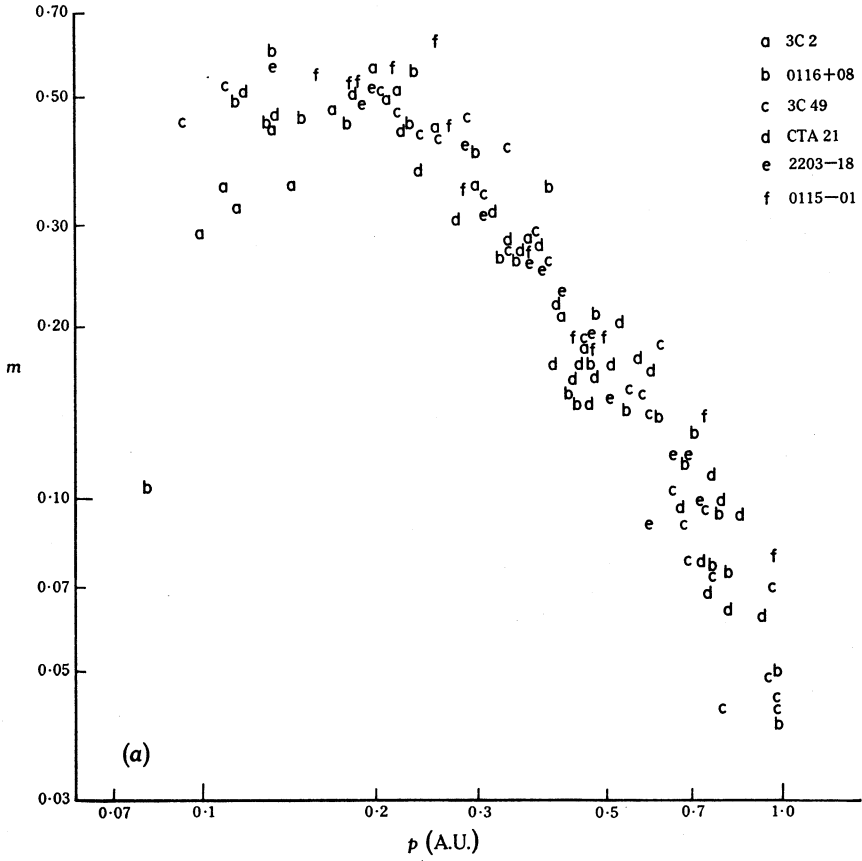


**Fig. 1.** Normalized scintillation indices  $m$  of the six unresolved sources:

(a) plotted as a function of elongation  $p$ , and

(b) averaged over small ranges of elongation in order to reduce the scatter.

The dashed curve in (b) is derived from the model described in Section 3.

effects of drifts and disturbances were minimized by using the 'phase-switched' mode, in which the output of one half of the telescope was multiplied with that of the other half. A bandwidth of 4 MHz was used for the observations and the output signal was smoothed with an  $RC$  time constant of 0.1 s. The data were sampled every 20 ms and recorded digitally on magnetic tape. The normal procedure was to record 6 min of data with the telescope pointing at the source and 3 min with the telescope pointing away. On many occasions, however, longer stretches of data were recorded. Sources were observed over elongations ranging from 0.05 to 1 A.U., but the results outside the range 0.1–0.7 A.U. are not very reliable because for  $p < 0.1$  A.U. the effect of the Sun in the side lobes made observations difficult while for  $p > 0.7$  A.U. the scintillations were very weak. Running means over 10 s were subtracted from the data to remove drifts and the variance  $\sigma^2$  of the data was computed. The scintillation index  $m$  was calculated from the definition

$$m = (\sigma_{\text{ON}}^2 - \sigma_{\text{OFF}}^2)^{1/2} / D,$$

where  $D$  is the deflection. This index is an underestimate because the high frequencies in the fluctuations are attenuated by the time constant. The amount of attenuation was estimated from the power spectrum and the scintillation index was corrected for it. This correction is around 10% for  $p > 0.2$  A.U. but increases at smaller elongations where the power spectrum becomes broad.

In Fig. 1*a* we have plotted the scintillation indices of the six unresolved sources against  $p$ . The indices of all the sources have been multiplied by a scaling factor to make the average  $m$ - $p$  curve for the source roughly coincide with that of CTA 21, which was taken to be a standard point source. The scaling factors are given in Table 1. There is considerable scatter in the indices which may be due to genuine changes in the properties of the interplanetary medium. In Fig. 1*b* the same data are shown averaged over small ranges of elongation in order to reduce the scatter. We see that for  $0.3 < p < 0.7$  A.U. there is a power law relation between  $m$  and  $p$  given by

$$m = 0.056 p^{-1.6}. \quad (1)$$

Outside this range the scintillation indices have values smaller than those given by the power law.

The power spectra of the data were computed using the fast Fourier algorithm. Running means over 10 s were subtracted from the data, the ends of the data were tapered with a cosine bell and the Fourier transform was computed. The Fourier coefficients were squared to give the power spectrum and block averages of four adjacent points were taken to give an effective resolution of  $25/256 \approx 0.1$  Hz. The spectra of successive minutes of data were cumulatively added. The power spectrum was then divided by the time constant pattern to correct for the attenuation. The spectrum of the receiver noise, which was a constant and independent of frequency after these manipulations, was subtracted from the measured spectrum for the on-source data to give the true spectrum of the intensity fluctuations. Since 6 min of data were normally taken, the statistical uncertainty in the spectrum was around 20% for small frequencies, where the power was large, and the uncertainty increased as the scintillation power level approached the receiver noise power level. Fig. 2 shows the computed power spectra of PKS 2203–18 for various elongations. It can be

seen that for  $p > 0.25$  A.U. the spectrum is roughly Gaussian but at smaller elongations the shape of the spectrum becomes exponential.

An estimate of the width of the power spectrum was made by computing the second moment  $f_2$  using the definition

$$f_2^2 = \int_0^{f_c} f^2 P(f) df / \int_0^{f_c} P(f) df,$$

where  $f_c$  is the frequency at which the scintillation power roughly becomes zero. In Fig. 3a we have plotted the second moments of the six sources whose moments are similar to that of CTA 21. The second moments of the three sources NRAO 91, 3C 138 and 3C 446, which have been omitted from Fig. 3a, seem to be affected by finite source size. The moments for the six sources show fluctuations from day to day and the average  $f_2$ - $p$  curve is given in Fig. 3b. It is seen that on the average  $f_2$  remains constant at about 0.6 Hz for  $p > 0.25$  A.U. but increases sharply at smaller elongations.

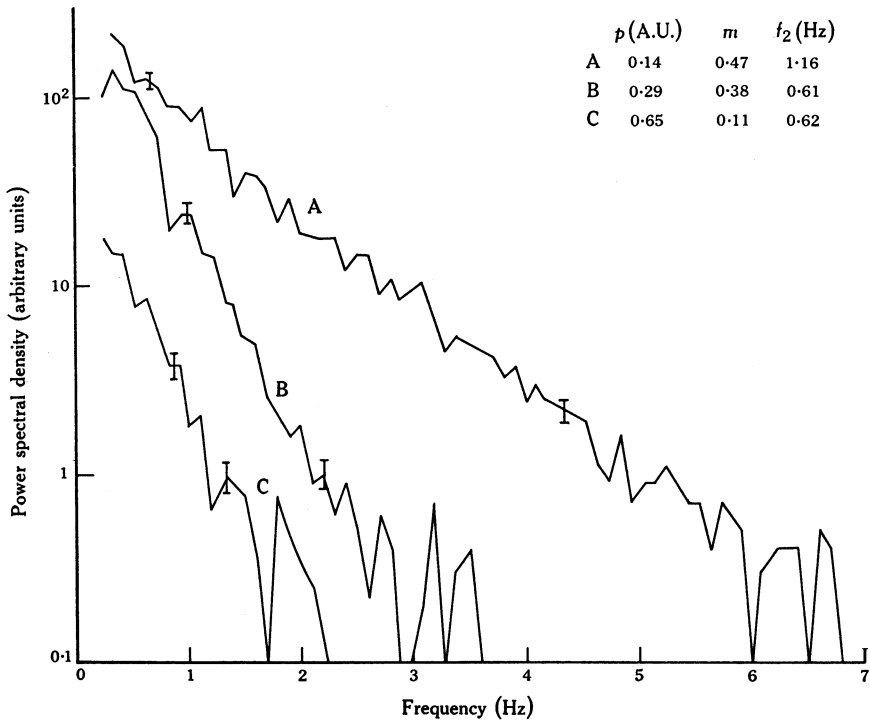
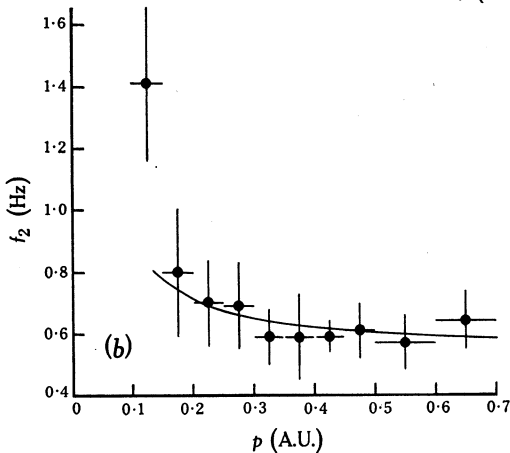
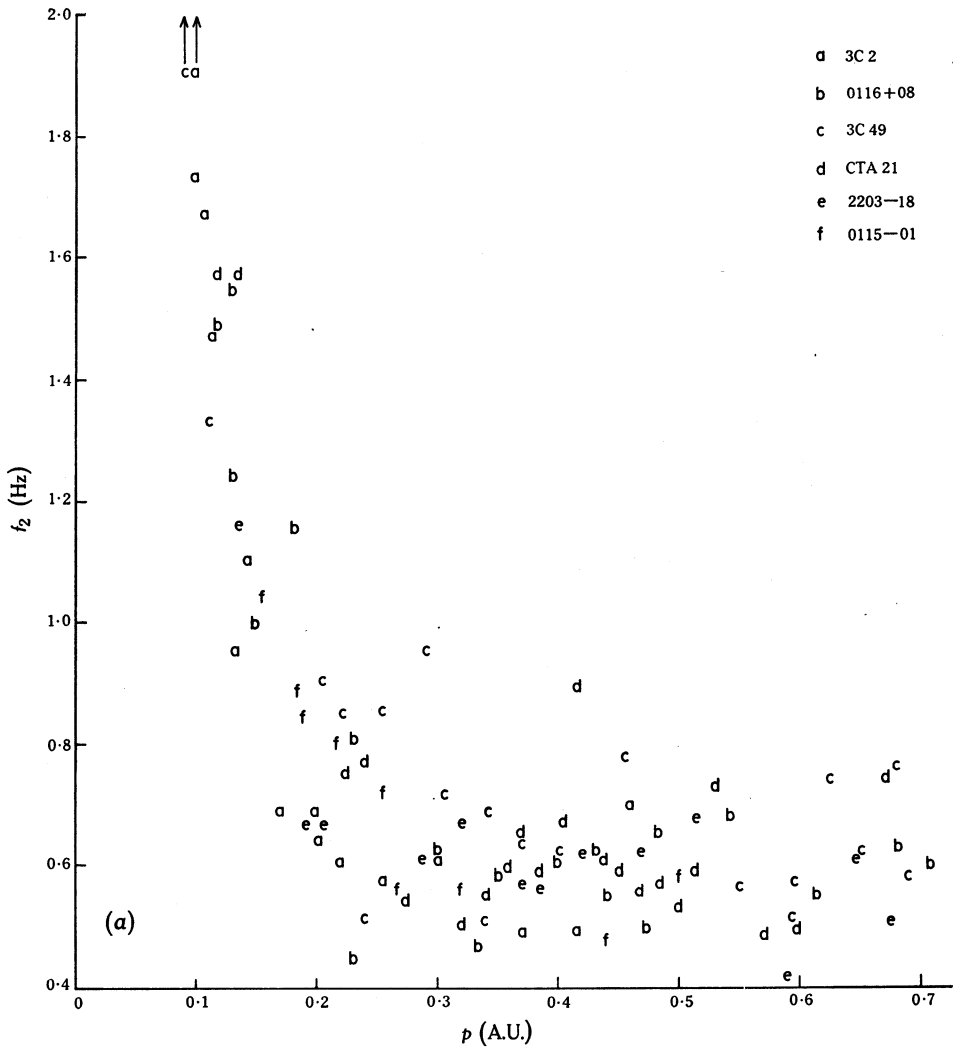


Fig. 2. Computed power spectra for PKS 2203-18 at three different elongations.

### 3. R.M.S. Phase Fluctuations and Scale Sizes

The scintillation index  $m$  and the second moment  $f_2$  depend upon the r.m.s. phase fluctuation  $\phi_0$  produced by the interplanetary medium along the line of sight to the source and the scale size  $a$  of the irregularities. The observed values of  $m$  and  $f_2$  can be compared with the theoretical values to obtain estimates of  $\phi_0$  and  $a$ . The theory of IPS has been discussed in detail by Salpeter (1967), and the theoretical



**Fig. 3.** Second moments  $f_2$  of the power spectra of the six unresolved sources:

(a) plotted as a function of elongation  $p$ , and  
 (b) averaged over small ranges of elongation.

The curve in (b) is derived from the model described in Section 3.

results used here can be derived directly from the expressions given by him. We will, unless otherwise specified, use the two-dimensional thin screen model and assume that the autocorrelation function of the phase fluctuations is a circularly symmetric Gaussian of the form

$$\rho(x, y) = \exp\{-(x^2 + y^2)/2a^2\}.$$

The discussion will be divided into two parts: in the first part we will estimate the parameters of the screen for  $p > 0.25$  A.U. where the scattering is clearly weak, that is,  $\phi_0 \ll 1$  rad, and the theory explains the observed quantities fairly well; in the second part we will compare theory and observation for  $p < 0.25$  A.U. and discuss the features which are not fully understood.

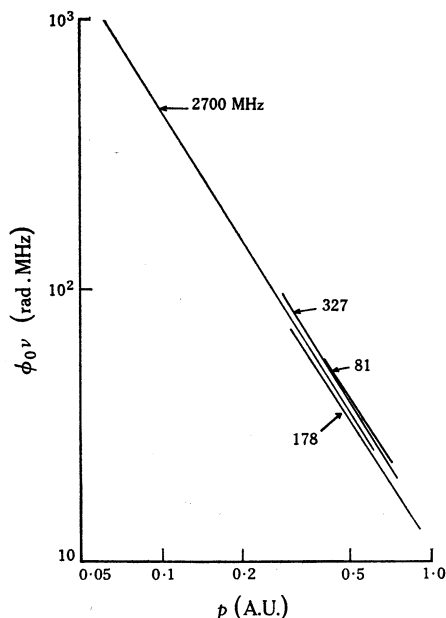


Fig. 4. Plots of  $\phi_0 \nu$  against elongation  $p$ . The present data at 327 MHz are compared with curves at 2700, 178 and 81 MHz taken from Little (1971).

$p > 0.25$  A.U.

For  $p > 0.25$  A.U. we are in the weak scattering regime where the scintillation index is given by

$$m = \sqrt{2} \phi_0 / \{1 + (\pi a^2 / \lambda z)^2\}^{\frac{1}{2}},$$

in which  $\lambda$  is the wavelength and the distance  $z$  of the observer from the thin screen is given by  $(1 - p^2)^{\frac{1}{2}}$  A.U. As is shown below, the average scale size in this region is about 100 km and so the above expression can be approximated by  $m = \sqrt{2} \phi_0$  with less than 10% error. Using this relation and equation (1) of Section 2 we get

$$\phi_0(327 \text{ MHz}) = 0.04 p^{-1.6} \text{ rad.}$$

$\phi_0$  has been estimated by a number of authors at various frequencies  $\nu$ ; Fig. 4 shows a combined plot of  $\phi_0 \nu$  against  $p$ . The observations at different frequencies cover different ranges of elongations but it can be seen that the measured  $\phi_0 \nu$  varies continuously over the whole range of  $p$  from 0.05 to 1.0 A.U., which implies that  $\phi_0$

does indeed vary as  $v^{-1}$ . As pointed out by Hewish (1971) and Little (1971), this rules out the proposal by Jokipii and Hollweg (1970) that the power spectrum of the irregularities is a power law, since in their model the estimated  $\phi_0$  varies faster than  $v^{-1}$ .

In the weak scattering regime, for a thin screen with a Gaussian autocorrelation function for the irregularities, the power spectrum of the observed intensity fluctuations is given by

$$P(f) = (32\pi)^{\frac{1}{2}} a \phi_0^2 v^{-1} \exp\{-0.5(2\pi af/v)^2\} \left(1 - \frac{\cos(\frac{1}{2}\theta + 2\pi\lambda z f^2/v^2)}{\{1 + (\lambda z/\pi a^2)^2\}^{1/4}}\right), \quad (2)$$

where  $\theta = \arctan(\lambda z/\pi a^2)$  and  $v$  is the velocity of the solar wind. Using equation (2), we get the following expression for  $f_2$ :

$$f_2 = (v/2\pi a)[1 + 2/\{1 + (\lambda z/\pi a^2)^2\}]^{\frac{1}{2}}.$$

In the far field region where  $z \gg \pi a^2/\lambda$ , this reduces to

$$f_2 = v/2\pi a.$$

Assuming that  $v = 350 \text{ km s}^{-1}$  in the range  $0.3 < p < 0.7 \text{ A.U.}$  and that we are in the far field region, the observed constant value of  $f_2$  at  $0.6 \text{ Hz}$  (Fig. 3b) implies a constant scale size of about  $100 \text{ km}$ . With this scale size the correction due to near-field effects is less than  $10\%$  for  $p < 0.7 \text{ A.U.}$  and can be neglected.

For large values of  $p$  the thin screen model may not be adequate since the thickness of the interplanetary medium affecting the observations becomes comparable with the distance to the effective thin screen. To be more realistic we should consider the fact that the different layers are at different distances from the observer and that the projected component of the solar wind velocity varies from layer to layer. We have therefore computed  $m$  and  $f_2$  for a spherically symmetrical interplanetary medium assuming it can be treated as a number of independent thin layers. The irregularities were also taken to be spherically symmetrical and to have a Gaussian autocorrelation function. The solar wind was assumed to have a constant velocity of  $350 \text{ km s}^{-1}$  for  $r > 0.3 \text{ A.U.}$ , where  $r$  is the radial distance from the Sun. The r.m.s. phase fluctuation  $F$  produced by unit length of the interplanetary medium and the scale size  $a$  were assumed to have the forms

$$F(r) = Ar^{-2}, \quad a(r) = Br^\alpha,$$

where values of  $A$ ,  $B$  and  $\alpha$  were determined as described below.

The scintillation index was estimated by computing the sum

$$m^2 = \sum_i 2F^2(r_i) dz^2/(1 + y_i^{-1}),$$

where

$$y_i = \{\lambda z_i/\pi a^2(r_i)\}^2$$

and  $dz$  is the thickness of each screen. The power spectrum is given by

$$P(f) = \sum_i P_i(f),$$

where  $P_i(f)$  is the power spectrum produced by the  $i$ th screen. Substituting for  $P_i(f)$  from equation (2), we derive the following expression for the second moment

$$f_2^2 = (2/m^2)dz^2 \sum_i v_i^2 F^2(r_i) y_i(3+y_i)/\{2\pi a_i(1+y_i)\}^2,$$

where  $v_i$  is the component of the solar wind velocity perpendicular to the line of sight at the  $i$ th screen. Various values of  $B$  and  $\alpha$  were tried until the model gave  $m$  and  $f_2$  comparable with the observed values. The data could be adequately fitted with any value of  $\alpha$  between 0.1 and 0.25 but we have taken  $\alpha = 0.25$  since this describes the  $f_2$ - $p$  curve down to  $p = 0.15$  A.U. The best fitting values of  $F(r)$  and  $a(r)$  were

$$F(r) = 3.56 \times 10^{-2} r^{-2} \text{ rad A.U.}^{-1}, \quad a(r) = 100 r^{0.25} \text{ km},$$

with  $r$  in A.U. The  $m$ - $p$  and  $f_2$ - $p$  curves given by the above model are shown in Figs 1b and 3b respectively.

The main uncertainty in such a calculation as described above is that the solar wind velocity and its radial dependence are not well known. Theoretical models for the solar wind indicate that the velocity increases weakly with  $r$ , for  $r > 0.2$  A.U., but the velocity measured using three-station observations of IPS (Vitkevich and Vlasov 1970) show no such effect in the range  $0.3 < r < 0.8$  A.U. Another source of uncertainty arises from the fact that we have assumed that  $a(r)$  and  $F(r)$  preserve their forms out to 3 or 4 A.U. from the Sun. No measurements of these quantities exist for  $r > 1$  A.U.

In the range  $0.35 < p < 0.8$  A.U. the scale size of the irregularities and the velocity of the solar wind have been directly measured using three-station IPS observations at around 80 MHz. Hewish and Symonds (1969) and Vitkevich and Vlasov (1970) have observed the source 3C48 while Armstrong and Coles (1972) have observed the compact source in the Crab nebula. The solar wind velocity measured by all observers does not show any marked variation with  $p$ . The scale sizes measured by Vitkevich and Vlasov and by Armstrong and Coles also do not show any variation with  $p$  and have a mean value of 150 and 200 km respectively. The scale size reported by Hewish and Symonds increases steeply with  $p$ , but these authors have assumed that 3C48 has a circularly symmetric Gaussian structure with diameter  $0''.3$  and have corrected the measured scale sizes for the diameter-blurring effects. The correction is based on a model which explains the observed turnover in the  $m$ - $p$  curve in terms of the finite diameter of the source. In this model the correction for the scale sizes is equal to the ratio of the observed value of  $m$  to that expected for an ideal point source. At 80 MHz 3C48 starts to turn over at  $p \approx 0.5$  A.U. and so the correction can be quite large for  $p < 0.5$  A.U. As the scintillation indices of all the sources observed at 327 MHz show turnover at  $p \approx 0.2$  A.U., this correction is not necessary for the scale sizes we have measured for  $p > 0.3$  A.U. The agreement between our measured dependence of the scale size on  $p$  with that found by Vitkevich and Vlasov suggests that the correction applied by Hewish and Symonds may not be necessary. In the next subsection we discuss the model on which the correction is based in more detail and show that it cannot be considered completely satisfactory.

At small elongations ( $0.05 < p < 0.3$  A.U.) the scale sizes have been determined by angular broadening measurements and by two-station IPS observations, and

these have been combined with the results of Hewish and Symonds (1969) at large  $p$  to get the general dependence of  $a$  on  $p$ . Little (1971) has found that the scale size varies as  $p^{0.9}$  in the range  $0.05 < p < 0.8$  A.U., while Readhead (1971) has assumed it to vary as  $r^{1.5}$ . Our measurements indicate that for  $r > 0.3$  A.U. these power law indices are too large. It seems rather unlikely that the relation between the scale size and  $r$  can be expressed as a single power law in the range  $0.05 < r < 1.0$  A.U. At least two power laws seem to be required: a flat one with index 0.2 for  $r > 0.3$  A.U. and a steeper one for smaller  $r$ .

$p < 0.25$  A.U.

In the region  $p < 0.25$  A.U. there are two features that are not clearly understood: one is the turnover in the  $m-p$  curve and the other is the change in the shape of the power spectrum from Gaussian to exponential. The theory of IPS predicts that as  $\phi_0$  increases  $m$  will also increase until it reaches a value of about 1, when  $m$  will then remain independent of  $\phi_0$ . It is observed, however, that the scintillation index saturates at values much smaller than 1 and close to the Sun it starts to decrease. At 327 MHz this turnover takes place at  $p$  slightly less than 0.2 A.U., where  $\phi_0$  is about 0.5 rad. Two processes which have been suggested to explain the turnover are the bandwidth effect (Little 1968) and the diameter-blurring effect (Little and Hewish 1966).

The receiver system has a finite coherence time because of its nonzero bandwidth, and this causes the angular spectra at large angles to the incident direction to become incoherent with respect to the spectra in the incident direction, thus reducing the scintillation index. The bandwidth decoherence becomes important when (Little 1968)

$$z\theta^2/2c \approx 1/\Delta\nu,$$

where  $\Delta\nu$  is the bandwidth,  $c$  is the velocity of light and  $\theta$  is the width of the angular spectrum which is given by

$$\begin{aligned} \theta &= \lambda/2\pi a & \text{for } \phi_0 \ll 1, \\ &= \lambda\phi_0/2\pi a & \phi_0 \gg 1. \end{aligned}$$

If this effect is responsible for the turnover then for a bandwidth of 4 MHz at 327 MHz the scale size at 0.2 A.U. should be about 6 km, and this is 5–10 times smaller than what is observed. It seems rather unlikely therefore that the turnover is due to the effect of the bandwidth.

In the diameter-blurring hypothesis the turnover in  $m$  is explained by the filtering out of the high frequencies in the power spectra due to the nonzero diameter of the source. If the source has a symmetrical Gaussian structure with diameter  $\theta_0$ , the measured scintillation index and the scale size are given by (Little and Hewish 1966)

$$m_{\text{obs}} = m_0 \{1 + 2(z\theta_0/a_0)^2\}^{-\frac{1}{2}}, \quad a_{\text{obs}} = a_0 \{1 + 2(z\theta_0/a_0)^2\}^{\frac{1}{2}}, \quad (3)$$

where  $m_0$  and  $a_0$  are the observed scintillation index and scale size for a point source;  $a_0 = a$  for  $\phi_0 \ll 1$  and  $a_0 = a/\phi_0$  for  $\phi_0 \gg 1$ . With decreasing elongation the term within braces in equations (3) increases faster than  $m_0$ , thus producing the turnover. It is observed that at a given frequency the scintillation indices of all the point sources

turn over at roughly the same  $p$ , where  $\phi_0 < 1$ , indicating that in the turnover region the effective scale size  $a_0$  is the same as the actual scale size  $a$  on the screen. It is also observed that at higher frequencies the turnover occurs closer to the Sun. In the diameter-blurring hypothesis these two observations can be explained only by assuming that all the so-called point sources have roughly the same finite angular diameter which increases as we go to lower frequencies. In fact, Harris *et al.* (1970) have suggested that the finite minimum diameter of sources could be caused by interstellar scattering. Assuming that the turnover occurs for  $z\theta_0/a \approx 1$ , we can estimate the minimum diameter if we know the scale sizes. Estimates by Little (1971) indicate that for  $p = 0.2$  A.U. the scale size is about 50 km, which would imply that the finite diameter  $\psi$  of sources at 327 MHz is  $2.34\theta_0 \approx 0''.15$ . This value seems rather unlikely since very long baseline interferometer (VLBI) measurements by Clarke *et al.* (1969) indicate that at 408 MHz there are many sources with components as small as  $0''.01$ . The observed turnover at 327 MHz for  $p \approx 0.2$  A.U. would imply that all the compact sources observed are either simple sources with diameter  $\approx 0''.15$  or are complex and consist of two or more compact components.

Another difficulty with the diameter-blurring hypothesis for the turnover is that we do not see the effect of the source structure on the power spectra. For a simple Gaussian structure, and for  $p$  less than the turnover value, the observed scale size is determined essentially by the diameter of the source and has a value  $\sqrt{2}z\theta_0$ . Below the turnover, therefore,  $f_2$  should saturate at some constant value. Our observations, however, indicate that  $f_2$  increases sharply with decreasing elongation and shows no sign of saturating. If the source is complex and consists of two or three point components we should find modulation in the power spectra, but this also has not been seen. It is therefore difficult to reconcile the behaviour of the power spectrum with the simple diameter-blurring hypothesis.

The shape of the power spectrum changes from Gaussian to exponential around the turnover region. If the spectrum of the phase fluctuation is Gaussian, we expect the power spectrum also to be roughly Gaussian, even in the strong scattering regime. Ekers and Little (1971) have tried to explain the observed exponential shape of the power spectrum in terms of turbulence in the solar wind, which they have measured and found important at distances less than 0.15 A.U. from the Sun. This explanation does not seem satisfactory, however, since at 327 MHz the transition from the Gaussian to exponential shape takes place at about 0.15 A.U., where the measured turbulence is small. Further, the measurements by Cohen and Gundermann (1969) at 11 and 21 cm indicate that at higher frequencies the transition takes place at smaller elongations. This frequency dependence of the transition point makes it rather unlikely that turbulence alone is responsible for the phenomenon. It seems more likely that the transition accompanies the onset of strong scattering, for which the thin screen model seems inadequate.

#### 4. Bessel Transform

In the theoretical expression for the power spectrum in equation (2) there is a modulation due to the cosine term which, if observed, can be used to estimate the velocity of the solar wind. It has been pointed out by Salpeter (1967) that the Bessel transform of the autocorrelation function of the intensity fluctuation has the form

$$P_B(f) = \Phi^2 \{ (2\pi f/v)^2 \} \sin^2(\pi \lambda z f^2 / v^2).$$

Here the amplitude of the modulation is much larger than in equation (2) and is more easily recognized. Lovelace *et al.* (1970) have calculated the Bessel transform for eight cases but only on three occasions were deep minima observed from which they could estimate the velocity of the solar wind. We have estimated the Bessel transforms for the sources observed here by calculating the Abel transform of the power spectrum. This method has the advantage that the correction for the effect of the time constant can be made before calculating the Abel transform. Further, since the power spectra had already been computed and stored, the amount of computer time required for this method was much less than for a direct computation of the Bessel transform. The first direct computations of the Abel transform did not give satisfactory results even when tried on noise-free functions with known transforms, but a modified form of the Abel transform which calculated the prewhitened Bessel transform  $fP_B(f)$  was found to be satisfactory. From the definition of the Abel transform, with some straightforward algebraic manipulation, one can show that

$$fP_B(f) = \frac{1}{\pi} \frac{d}{df} \left( \int_f^\infty dx (x^2 - f^2)^{\frac{1}{2}} dP_f(x)/dx \right).$$

This expression was used to calculate the Bessel transform of all the data. Power spectra with a resolution of 0.025 Hz were used for the computation and the Abel transforms were smoothed by taking running means to give a fairly stable spectrum with a resolution of 0.1 Hz.

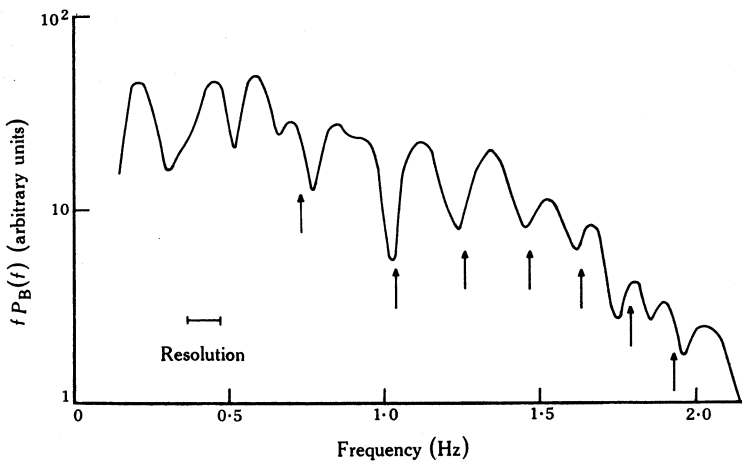


Fig. 5. Bessel transform for PKS 2203-18 from observations on 8 March 1971. The arrows indicate the positions of expected Fresnel minima.

Bessel transforms with  $\geq 9$  min of data gave satisfactory signal to noise ratios but even these spectra rarely showed minima at frequencies proportional to  $\sqrt{n}$ , as expected for Fresnel filtering. We have found interpretable deep minima only in 2 out of the 50 or so Bessel transforms computed. Fig. 5 shows the Bessel transform for the source PKS 2203-18, which was observed on 8 March 1971 at  $p = 0.37$  A.U. This transform shows five minima which are related approximately as  $\sqrt{n}$ ; the first minimum is at 0.75 Hz, giving  $v = 280 \text{ km s}^{-1}$  for  $z = 1$  A.U. On 6 May 1971,

the Bessel transform for the source PKS0115-01 at  $p = 0.5$  A.U. showed three deep minima related as  $\sqrt{n}$ , and gave  $v = 370 \text{ km s}^{-1}$ .

The absence of the spectral minima on most occasions is unlikely to be due to the finite resolution of the spectrum. At 327 MHz the first null in the Bessel transform is at

$$f_B = v/(z\lambda)^{\frac{1}{2}} = 0.9 \text{ Hz}$$

for  $v = 350 \text{ km s}^{-1}$  and  $z = 1$  A.U. Subsequent minima occur at  $\sqrt{n}f_B$  where  $n = 2, 3, \dots$ . With our resolution of 0.1 Hz we should have seen at least four or five minima if they had been present.

There are two effects which can reduce the amplitude of the modulation, and quantitative estimates of each have been given by Bourgois (1972). The first is that the irregularities may not be circularly symmetrical. If the irregularities are elongated in the direction of the velocity then the amplitude of the modulation in the Bessel transform is reduced. If we take the anisotropy ratio to be equal to two, which is close to what is observed, and take the scale size to be 120 km along the solar wind direction and 60 km in the perpendicular direction, then for  $z = 1$  A.U., using the expressions from Bourgois (1972), the amplitude of the modulation decreases from 100% to about 70%, which should still be observable. The other cause of the reduction of the modulation is the finite thickness of the screen. This causes the modulation to be blurred since both  $z$  and the component of  $v$  perpendicular to the line of sight vary across the screen. Numerical calculations by Ward *et al.* (1972) indicate that this effect should be relatively unimportant for elongations less than 0.5 A.U. It is therefore difficult to understand why for elongations less than this value the Fresnel filtering effect is not seen. It is possible that in addition to the systematic radial outflow of the solar wind there is a small random velocity field which smears out the modulation.

## 5. Skewness Parameter

An estimate of the skewness of the probability distribution of the intensity fluctuations was made by calculating a skewness parameter  $\gamma$  which, following Bourgois and Cheynet (1972), was defined as

$$\gamma = \langle (I - \bar{I})^3 \rangle / \langle (I - \bar{I})^2 \rangle^{3/2}.$$

The skewness parameter is a function of  $\phi_0$  but the actual functional form depends on the adopted model for the interplanetary medium. In the thin screen model the probability distribution is expected to be a Rice distribution, and for this Bourgois and Cheynet have shown that

$$\gamma = 2\{1 + 2\exp(-\phi_0^2)\}\{1 - \exp(-\phi_0^2)\}\{1 + \exp(-\phi_0^2)\}^{-3/2}.$$

For  $\phi_0 \ll 1$  we have

$$\gamma = (3/\sqrt{2})\phi_0 = 1.5m.$$

If now, instead of the thin screen model, the interplanetary medium is considered to be a uniform thick slab consisting of weakly scattering layers, the probability distribution for the intensity fluctuation is expected to be log-normal (Young 1971),

and for such a distribution

$$\gamma = 3m + m^3.$$

By studying the dependence of  $\gamma$  on  $m$  we can distinguish between the two models. In Fig. 6 the observed  $\gamma$  is plotted against the normalized scintillation index for the observed sources. Only observations for  $p > 0.2$  A.U. have been used since for smaller elongations  $m$  starts turning over. Also shown in the figure are the expected relations for the two models. It is seen that for small values of  $m$ , that is, at large distances from the Sun, the points are fairly uniformly scattered between the two curves. As we approach the Sun, and  $m$  increases, the observed points tend to be closer to the curve for the Rice distribution.

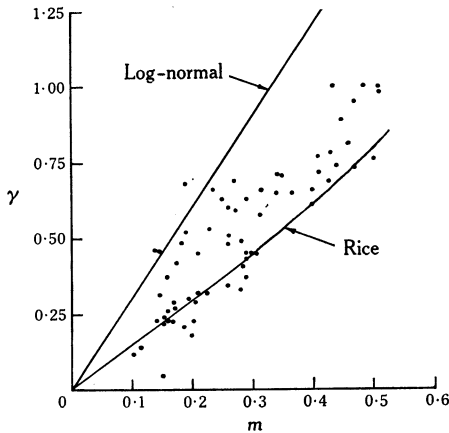


Fig. 6. Skewness parameter  $\gamma$  plotted against the normalized scintillation index  $m$  for the sources observed. The curves show the expected variations for Rice and log-normal probability distributions.

Observations of the skewness by Bourgois and Cheynet (1972) at 1410 MHz indicate that the intensity fluctuations have a Rice distribution for  $p < 0.15$ , except very close to the Sun, while the observations at 74 MHz by Armstrong *et al.* (1972) suggest that the intensity fluctuations can be much better represented by a log-normal distribution for  $p > 0.5$  A.U. Our observations at 327 MHz, which cover the range  $0.2 < p < 0.6$  A.U. indicate that the statistics of the intensity fluctuations lie between Rice and log-normal but tend more to Rice as  $p$  decreases. There seems to be a continuous transition from the thin screen model which is valid close to the Sun to the thick screen model which is valid at large distances. It is possible that the statistics of the intensity fluctuations could be described over the whole range of elongations by a realistic thick slab model in which the r.m.s. phase fluctuation produced by each layer depends on its distance from the Sun.

## 6. Source Structure

The structure of a radio source can be derived by comparing its scintillations with that of CTA 21, which is taken to be a point source. The ratio  $\mu$  of its scintillation index to that of CTA 21, at the same elongation, indicates if the source is a simple point source or has an extended non-scintillating halo around it. If the power spectrum of the source is similar to that of a point source, the value of  $\mu$  gives the ratio of the flux in the scintillating component to the total flux of the source. If, however, the power spectrum of the source is narrower than that of a point source,

we can estimate the diameter of the scintillating component using the formula given by Cohen *et al.* (1967),

$$\psi = (v/1.2\pi f_2 z)\{1 - (f_2/f_0)^2\}^{\frac{1}{2}},$$

where  $\psi$  is the half-power width of the source, which is assumed to be a Gaussian, and  $f_2$  and  $f_0$  are the second moments for the given source and for a point source respectively. For these resolved sources we can correct the observed scintillation index for the finite diameter of the source using the formula

$$m = m_{\text{obs}}\{1 + 0.36(z\psi/a)^2\}^{\frac{1}{2}},$$

where  $m$  and  $m_{\text{obs}}$  are the corrected and observed scintillation indices respectively. The corrected scintillation indices have been used in estimating the fraction of the flux in the scintillating component. For the resolved sources one can study the variation, if any, in the measured diameter as the position angle of the solar wind across the source varies and thus make models for the two-dimensional structure of the source.

**Table 1. Source structures derived from interplanetary scintillations at 327 MHz**

Source	Fraction of flux in compact component	Scaling factor used to normalize scintillation index	Angular diameter of scintillating component	Position angle (deg)
3C 2	0.6	1.6	$< 0''.06$	240
PKS 0115-01	1.0	0.9	$< 0''.1$	144
PKS 0116+08	0.75	1.3	$< 0''.08$	70
3C 49	0.75	1.3	$< 0''.06$	30
NRAO 91	1.0	0.8	$\sim 0''.1$	60*
CTA 21	1.0	1.0	$< 0''.08$	90
3C 138	1.0	1.1	$\sim 0''.25 \times < 0''.1$	—*
PKS 2203-18	1.0	1.0	$< 0''.1$	200
3C 446	1.0	1.1	$\sim 0''.25 \times < 0''.1$	—*

\* See comments in Section 6.

For the unresolved sources an upper limit to the diameter is given by

$$\psi \leq v/1.2\pi f_2 z.$$

The maximum value of  $f_2$  measured is about 2 Hz at  $p \approx 0.1$  A.U. and, assuming that  $v = 300 \text{ km s}^{-1}$  at this distance and that  $z = 1.0$  A.U., the upper limit on the diameter of the unresolved sources is about  $0''.06$ . Table 1 lists information on the derived structure for the nine sources observed. Comments on the structure of the three resolved sources are given below.

### 3C 446

The structure of 3C 446 varies with the position angle (p.a.) of the solar wind. At large elongations the p.a. is about  $260^\circ$ , and the values of  $f_2$  are consistently lower than those for a point source,  $\psi$  being estimated as  $\approx 0''.25$ . At small elongations, however, the p.a. changes by  $\sim 90^\circ$  and  $f_2$  increases as for a point source, setting an upper limit on  $\psi$  of  $0''.1$ . Similar results on the structure of this source have been reported by Miley *et al.* (1967) using interferometry at 21 cm.

### 3C138

This source also shows variation of diameter with p.a. It is extended along p.a.  $\approx 240^\circ$ , where it has  $\psi \approx 0''\cdot25$ . In the perpendicular direction the source remains unresolved. Our results agree reasonably with the structure found by Donaldson *et al.* (1971) at 2694 MHz, using VLBI with a baseline of  $1\cdot1 \times 10^6$  wavelengths. In addition to the elongated component seen by us, they have reported the presence of compact components with diameter  $< 0''\cdot04$ . It is possible that these components are self-absorbed and contribute very little flux at 327 MHz.

### NRAO 91

This source appears unresolved for large values of  $p$  but, for  $p < 0\cdot2$  A.U.,  $f_2$  does not increase as expected for an unresolved point source and gives  $\psi \approx 0''\cdot1$ . The VLBI measurements at high frequencies by Kellermann *et al.* (1971) give  $\psi \approx 0''\cdot001$ . It is possible that the structure of the source varies with frequency. The source is peculiar as its  $m$  value is generally higher than that of CTA 21, which is taken to be an ideal point source, and perhaps there is confusion with some nearby source.

## 7. Conclusions

From the present estimates of the r.m.s. phase fluctuations and the scale size of the irregularities in the interplanetary medium in the range of elongation  $0\cdot3 < p < 0\cdot7$  A.U., it has been found that the scale size is nearly independent of  $p$  and is about 100 km. This result does not agree with that of Hewish and Symonds (1969), who found that the scale size increased rapidly with  $p$ . The discrepancy may be due to their correction of the observed scale size for the finite diameter of the source, as well as the model used for the correction. Our observations do not need any corrections in the above range of elongations. An examination of the various explanations suggested for the observed decrease in the scintillation index close to the Sun has shown that they are not fully satisfactory. To understand the true cause of this turnover, it will be of value to study the low frequency structure of radio sources used for IPS observations with a resolution of better than  $\sim 0''\cdot1$ , as can be done by very long baseline interferometry.

The Bessel transforms of the intensity fluctuations have been computed to determine, if possible, the solar wind velocity from our single antenna observations. The deep minima due to the Fresnel filtering effect were rarely present and this shows that the ideal thin screen theory may not be adequate.

The study of the skewness parameter of the probability distribution of the intensity fluctuations has indicated that for elongations less than about 0·35 A.U. the distribution is better approximated by a Rice distribution than a log-normal one, but for larger elongations it is difficult to choose between the two.

## Acknowledgments

We thank Professor G. Swarup, Mr V. K. Kapahi and Professor T. K. Menon for reading the manuscript and making many helpful comments. One of us (S.M.B.) is grateful to Professor U. R. Rao for encouragement and to the Department of Space, Government of India, for financial assistance.

## References

- Armstrong, J. W., and Coles, W. A. (1972). *J. geophys. Res.* **77**, 4602.
- Armstrong, J. W., Coles, W. A., and Rickett, B. J. (1972). *J. geophys. Res.* **77**, 2739.
- Bhandari, S. M., Ananthakrishnan, S., and Rao, A. Pramesh (1974). *Aust. J. Phys.* **27**, 121.
- Bourgois, G. (1972). *Astr. Astrophys.* **19**, 200.
- Bourgois, G., and Cheynet, C. (1972). *Astr. Astrophys.* **21**, 25.
- Clarke, R. W., Broten, N. W., Legg, T. H., Locke, J. L., and Yen, J. L. (1969). *Mon. Not. R. astr. Soc.* **146**, 381.
- Cohen, M. H., and Gundermann, E. J. (1969). *Astrophys. J.* **155**, 645.
- Cohen, M. H., Gundermann, E. J., and Harris, D. E. (1967). *Astrophys. J.* **150**, 767.
- Donaldson, W., Miley, G. K., and Palmer, H. P. (1971). *Mon. Not. R. astr. Soc.* **152**, 145.
- Ekers, R. D., and Little, L. T. (1971). *Astr. Astrophys.* **10**, 310.
- Harris, D. E., Zeissig, G. A., and Lovelace, R. V. (1970). *Astr. Astrophys.* **8**, 98.
- Hewish, A. (1971). *Astrophys. J.* **163**, 645.
- Hewish, A., and Symonds, M. D. (1969). *Planet. Space Sci.* **17**, 313.
- Jokipii, J. R., and Hollweg, J. V. (1970). *Astrophys. J.* **160**, 745.
- Kellermann, K. I., *et al.* (1971). *Astrophys. J.* **169**, 1.
- Little, L. T. (1968). *Planet. Space Sci.* **16**, 749.
- Little, L. T. (1971). *Astr. Astrophys.* **10**, 301.
- Little, L. T., and Hewish, A. (1966). *Mon. Not. R. astr. Soc.* **134**, 221.
- Lovelace, R. V. E., Salpeter, E. E., Sharp, L. E., and Harris, D. E. (1970). *Astrophys. J.* **159**, 1047.
- Miley, G. K., Rickett, B. J., and Gent, H. (1967). *Nature* **216**, 974.
- Readhead, A. C. S. (1971). *Mon. Not. R. astr. Soc.* **155**, 185.
- Salpeter, E. E. (1967). *Astrophys. J.* **147**, 433.
- Swarup, G., *et al.* (1971). *Nature Phys. Sci.* **230**, 185.
- Vitkevich, V. V., and Vlasov, V. I. (1970). *Soviet Astr.* **13**, 669.
- Ward, B. D., Blesing, R. G., and Dennison, P. A. (1972). *Proc. astr. Soc. Aust.* **2**, 82.
- Young, A. T. (1971). *Astrophys. J.* **168**, 543.